CPC(HEP & NP), 2009, **33**(9): 722—728 Chinese Physics C Vol. 33, No. 9, Sep., 2009

$B \to \pi\eta^{(\prime)}$, $\eta^{(\prime)}\eta^{(\prime)}$ decays and NLO contributions in the pQCD approach*

ZHANG Zhi-Qing(张志清)[1)]LIU Xin(刘新)[2)] XIAO Zhen-Jun(肖振军)[3)]

(Department of Physics and Institute of Theoretical Physics, Nanjing Normal University, Nanjing 210097, China)

Abstract By employing the perturbative QCD (pQCD) factorization approach, we calculate the full leading and the partial next-to-leading order (NLO) contributions to the seven $B \to \pi\eta^{(\prime)}$ and $\eta^{(\prime)}\eta^{(\prime)}$ decays. For $B^+ \to \pi^+\eta^{(\prime)}$ decays, the pQCD predictions for their decay rates agree very well with the data after the inclusion of the small NLO contributions. For neutral decays, the pQCD predictions are also consistent with the experimental upper limits and can be tested by the LHC experiments. The measured value of $\mathcal{A}_{CP}^{\rm dir}(\pi^{\pm}\eta) = -19\pm7\%$ can also be accommodated by the pQCD approach.

Key words B meson decay, the pQCD factorization approach, branching ratio

PACS 13.25.Hw, 12.38.Bx, 14.40.Nd

1 Introduction

The two body charmless hadronic B meson decays involving the $\eta^{(\prime)}$ mesons as the one or even two final state mesons are very interesting phenomenologically, because of the well-known $K\eta'$ puzzle and the possible gluonic component of the flavor singlet η and η'[1, 2].

In this paper, we would like to calculate the branching ratios and CP asymmetries for the seven $B \to \pi\eta^{(\prime)}$ and $B \to \eta^{(\prime)}\eta^{(\prime)}$ decays, by employing the pQCD approach with the inclusion of the full leading order (LO) and the partial NLO contributions. These seven decay modes have been studied before in the generalized factorization approach[3], in the QCD factorization (QCDF) approach[4—6], and in the pQCD approach at the LO level[7, 8]. Here we will focus on the evaluation of the partial NLO contributions from the vertex corrections, the quark-loops and the chromo-magnetic penguins[2, 9].

The paper is organized as follows. In Sec. 2, we firstly re-calculate the leading order Feynman diagrams, and then evaluate the partial NLO contributions. In Sec. 3, we calculate and show the pQCD predictions for the branching ratios and CP violating asymmetries of the seven $B \to \pi\eta^{(\prime)}, \eta^{(\prime)}\eta^{(\prime)}$ decays. The summary and some discussions are also included in this section.

2 Calculations in the PQCD approach

2.1 Theoretical framework

In the light-cone coordinate, the B meson and the two final state meson momenta can be written as

$$\begin{aligned} P_1 &= \frac{M_B}{\sqrt{2}}(1,1,\mathbf{0}_T), \\ P_2 &= \frac{M_B}{\sqrt{2}}(1,0,\mathbf{0}_T), \\ P_3 &= \frac{M_B}{\sqrt{2}}(0,1,\mathbf{0}_T), \end{aligned} \tag{1}$$

respectively. Here the light meson $\pi, \eta^{(\prime)}$ masses have been neglected. Putting the light anti-quark momenta in B, and two mesons π (or $\eta^{(\prime)}$), $\eta^{(\prime)}$ as k_1, k_2 and k_3, respectively, we can choose

$$\begin{aligned} k_1 &= (x_1 P_1^+, 0, \boldsymbol{k}_{1T}), \\ k_2 &= (x_2 P_2^+, 0, \boldsymbol{k}_{2T}), \\ k_3 &= (0, x_3 P_3^-, \boldsymbol{k}_{3T}). \end{aligned} \tag{2}$$

Received 9 January 2009, Revised 4 February 2009

* Supported by National Natural Science Foundation of China (10575052, 10735080) and Specialized Research Fund for Doctoral Program of Higher Education (SRFDP) (20050319008)

1) E-mail: zhangzhiqing@zzu.edu.cn

2) E-mail: hsinlau@126.com

3) E-mail: xiaozhenjun@njnu.edu.cn

Then, the decay amplitude is factorized into the convolution of the mesons' wave functions $\Phi_B(x_1,b_1)$ and $\Phi_{M_i}(x_i,b_i)$, the hard scattering kernel $H(x_i,b_i,t)$, the Wilson coefficients $C_i(t)$ and the Sudakov form factor $S_t(x_i)$,

$$\mathcal{A}(B\to M\eta^{(\prime)}) \sim \int dx_1 dx_2 dx_3 b_1 db_1 b_2 db_2 b_3 db_3 \times \mathrm{Tr}\left[C(t)\Phi_B(x_1,b_1)\Phi_M(x_2,b_2)\times \Phi_{\eta^{(\prime)}}(x_3,b_3)H(x_i,b_i,t)S_t(x_i)\,e^{-S(t)}\right], \quad (3)$$

where b_i is the conjugate space coordinate of the transverse momentum k_{iT}, and t is the largest energy scale in function $H(x_i,b_i,t)$.

The B meson is as usual treated as a heavy-light system. We use the same wave function as in Refs. [10, 11]:

$$\Phi_B = \frac{1}{\sqrt{2N_c}}(\not{P}_B + m_B)\gamma_5\phi_B(\boldsymbol{k}_1). \quad (4)$$

For the π meson, we use the same wave function $\Phi_\pi(x)$, the twist-2 pion distribution amplitude (DA) ϕ_π^A, and the twist-3 ones ϕ_π^P and ϕ_π^T as in Ref. [7]. For the η-η' system, we also use the quark-flavor mixing scheme, where the physical states η and η' are related to the flavor states $\eta_q=(u\bar{u}+d\bar{d})/\sqrt{2}$ and $\eta_s=s\bar{s}$ through a single mixing angle ϕ. The explicit expressions of the mixing matrix, the wave functions of Φ_{η_q} and Φ_{η_s}, the twist-2 and twist-3 DA's $\phi_{\eta_q}^{A,P,T}(x_i)$ and $\phi_{\eta_s}^{A,P,T}(x_i)$, can be found for example in Ref. [2].

2.2 Leading-order decay amplitudes

For $B\to\pi\eta^{(\prime)}$, $\eta^{(\prime)}\eta^{(\prime)}$ decays, the related weak effective Hamiltonian $\mathcal{H}_{\rm eff}$ for the $b\to d$ transition can be written as[12]

$$\mathcal{H}_{\rm eff} = \frac{G_F}{\sqrt{2}}\left\{\sum_{q=u,c} V_{qb}V_{qd}^*\left[C_1(\mu)O_1^q(\mu) + C_2(\mu)O_2^q(\mu)\right] - V_{tb}V_{td}^*\sum_{i=3}^{10}C_i(\mu)\,O_i(\mu)\right\}, \quad (5)$$

where $G_F = 1.16639\times10^{-5}$ GeV^{-2} is the Fermi constant, V_{ij}'s are the Cabbibo-Kobayashi-Maskawa (CKM) mixing matrix elements, $C_i(\mu)$ are the Wilson coefficients and $O_i(\mu)$ are the 4-Fermi "current-current" and penguin operators[12].

The LO Wilson coefficients $C_i(M_W)$ are simple and can be found easily in Ref. [12]. The LO renormalization group (RG) evolution matrix $U(t,m)$ from the high scale m down to $t(<m)$ can be found in Eq. (3.94) in Ref. [12]. When the NLO contributions are taken into account, the NLO Wilson coefficients $C_i(m_W)$ and RG evolution matrix $U(t,m,\alpha)$ are needed and can also be found in Ref. [12].

The important and difficult task is the calculation of the hard part $H(t)$. This part involves the four quark operators and the necessary hard gluon connecting the four quark operators and the spectator quark. For $B\to\pi\eta^{(\prime)}$ decays, for example, there are 8 types of the Feynman diagrams contributing to them, as illustrated in Fig. 1. The explicit amplitudes $F_{e\pi}$, $F_{e\pi}^{P1}$ and $F_{e\pi}^{P2}$ are coming from Fig. 1(a) and 1(b) for the case of $\eta^{(\prime)}$-emission, while $M_{e\pi}$ and $M_{e\pi}^{P1,P2}$ are coming from Fig. 1(c) and 1(d). The decay amplitudes $F_{a\pi}, F_{a\pi}^{P1,P2}$ and $M_{a\pi}, M_{a\pi}^{P1,P2}$ are obtained by evaluating the four annihilation diagrams.

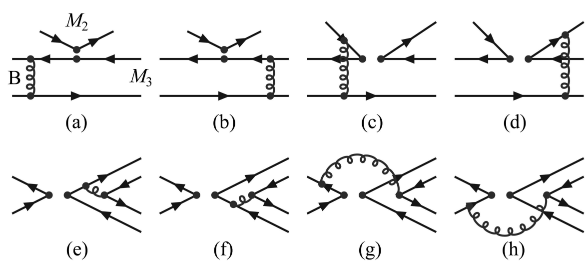

Fig. 1. The typical Feynman diagrams contributing to the $B\to\pi\eta^{(\prime)}$, $\eta\eta$, $\eta\eta'$ and $\eta'\eta'$ decays. Diagram (a) and (b) contribute to the form factors $F_{0,1}^{B\to\pi}$ and $F_{0,1}^{B\to\eta^{(\prime)}}$.

For these decays, by combing the contributions from different diagrams, it is easy to write out the total decay amplitudes at the leading order.

$$\begin{aligned}\mathcal{M}(\pi^+\eta) =\ & F_{e\pi}\left\{\left[\xi_u a_2 - \xi_t\left(2a_3+a_4-2a_5-\frac{a_7}{2}+\frac{a_9}{2}-\frac{a_{10}}{2}\right)\right]f_\eta^d - \xi_t\left(a_3-a_5+\frac{a_7}{2}-\frac{a_9}{2}\right)f_\eta^s\right\} - \\ & F_{e\pi}^{P2}\xi_t\left(a_6-\frac{1}{2}a_8\right)f_\eta^d + F_{e\eta}\left[\xi_u a_2 - \xi_t(a_4+a_{10})\right]f_\pi F_1(\phi) + \\ & M_{e\pi}F_1(\phi)\left\{\left[\xi_u C_2 - \xi_t\left(C_3+2C_4-\frac{1}{2}C_9+\frac{1}{2}C_{10}\right)\right]F_1(\phi) - \xi_t\left(C_4-\frac{1}{2}C_{10}\right)F_2(\phi)\right\} - \\ & (M_{a\eta}^{P1}+M_{a\pi}^{P1})\xi_t\,(C_5+C_7)\,F_1(\phi) - M_{e\pi}^{P2}\xi_t\left[\left(2C_6+\frac{1}{2}C_8\right)F_1(\phi) + \left(C_6-\frac{1}{2}C_8\right)F_2(\phi)\right] + \\ & (M_{a\pi}+M_{e\eta}+M_{a\eta})\left[\xi_u C_1 - \xi_t\,(C_3+C_9)\right]F_1(\phi) - \left(F_{a\pi}^{P2}+F_{a\eta}^{P2}\right)\xi_t\,(a_6+a_8)\,F_1(\phi), \end{aligned} \quad (6)$$

$$\begin{aligned}
\sqrt{2}\mathcal{M}(\pi^0\eta) = {} & F_{\mathrm{e}\eta}\left[\xi_{\mathrm{u}}a_2-\xi_{\mathrm{t}}\left(-a_4-\frac{3}{2}a_7+\frac{3}{2}a_9+\frac{1}{2}a_{10}\right)\right]f_\pi F_1(\phi)- \\
& F_{\mathrm{e}\pi}\left\{\left[\xi_{\mathrm{u}}a_2-\xi_{\mathrm{t}}\left(2a_3+a_4-2a_5-\frac{a_7}{2}+\frac{a_9}{2}-\frac{a_{10}}{2}\right)\right]f_\eta^{\mathrm{d}}-\xi_{\mathrm{t}}\left(a_3-a_5+\frac{a_7}{2}-\frac{a_9}{2}\right)f_\eta^{\mathrm{s}}\right\}+ \\
& F_{\mathrm{e}\pi}^{P2}\xi_{\mathrm{t}}\left(a_6-\frac{1}{2}a_8\right)f_\eta^{\mathrm{d}}-M_{\mathrm{e}\pi}F_1(\phi)\left\{\left[\xi_{\mathrm{u}}C_2-\xi_{\mathrm{t}}\left(C_3+2C_4-\frac{1}{2}C_9+\frac{1}{2}C_{10}\right)\right]F_1(\phi)-\right. \\
& \left.\xi_{\mathrm{t}}\left(C_4-\frac{1}{2}C_{10}\right)F_2(\phi)\right\}+(M_{\mathrm{a}\eta}^{P1}+M_{\mathrm{a}\pi}^{P1})\xi_{\mathrm{t}}\left(C_5-\frac{1}{2}C_7\right)F_1(\phi)+ \\
& M_{\mathrm{e}\pi}^{P2}\xi_{\mathrm{t}}\left[\left(2C_6+\frac{1}{2}C_8\right)F_1(\phi)+\left(C_6-\frac{1}{2}C_8\right)F_2(\phi)\right]+ \\
& (M_{\mathrm{a}\pi}+M_{\mathrm{e}\eta}+M_{\mathrm{a}\eta})\left[\xi_{\mathrm{u}}C_2-\xi_{\mathrm{t}}\left(-C_3+\frac{1}{2}C_9+\frac{3}{2}C_{10}\right)\right]F_1(\phi)- \\
& \frac{3}{2}(M_{\mathrm{a}\pi}^{P2}+M_{\mathrm{e}\eta}^{P2}+M_{\mathrm{a}\eta}^{P2})\xi_{\mathrm{t}}C_8F_1(\phi)+F_{\mathrm{e}\pi}^{P2}\xi_{\mathrm{t}}\left(a_6-\frac{1}{2}a_8\right)F_1(\phi),
\end{aligned} \tag{7}$$

$$\begin{aligned}
\mathcal{M}(\eta\eta') = {} & \left(F_{\mathrm{e}\eta}F_1(\phi)f_{\eta'}^{\mathrm{d}}+F_{\mathrm{e}\eta'}F_1'(\phi)f_\eta^{\mathrm{d}}\right)\cdot\left[\xi_{\mathrm{u}}a_2-\xi_{\mathrm{t}}\left(2a_3+a_4-2a_5-\frac{a_7}{2}+\frac{a_9}{2}-\frac{a_{10}}{2}\right)\right]- \\
& \left(F_{\mathrm{e}\eta}F_1(\phi)f_{\eta'}^{\mathrm{s}}+F_{\mathrm{e}\eta'}F_1'(\phi)f_\eta^{\mathrm{s}}\right)\xi_{\mathrm{t}}\left(a_3-a_5+\frac{a_7}{2}-\frac{a_9}{2}\right)- \\
& \left(F_{\mathrm{e}\eta}^{P2}F_1(\phi)f_{\eta'}^{\mathrm{d}}+F_{\mathrm{e}\eta'}^{P2}F_1'(\phi)f_\eta^{\mathrm{d}}\right)\xi_{\mathrm{t}}\left(a_6-\frac{1}{2}a_8\right)+ \\
& (M_{\mathrm{e}\eta}+M_{\mathrm{e}\eta'})F_1(\phi)F_1'(\phi)\left[\xi_{\mathrm{u}}C_2-\xi_{\mathrm{t}}\left(C_3+2C_4-\frac{1}{2}C_9+\frac{1}{2}C_{10}\right)\right]- \\
& [M_{\mathrm{e}\eta}F_1(\phi)F_2'(\phi)+M_{\mathrm{e}\eta'}F_1'(\phi)F_2(\phi)]\xi_{\mathrm{t}}\left(C_4-\frac{1}{2}C_{10}\right)- \\
& \left(M_{\mathrm{e}\eta}^{P2}+M_{\mathrm{e}\eta'}^{P2}\right)F_1(\phi)F_1'(\phi)\xi_{\mathrm{t}}\left(2C_6+\frac{1}{2}C_8\right)- \\
& \left(M_{\mathrm{e}\eta}^{P2}F_1(\phi)F_2'(\phi)+M_{\mathrm{e}\eta'}^{P2}F_1'(\phi)F_2(\phi)\right)\xi_{\mathrm{t}}\left(C_6-\frac{1}{2}C_8\right)+ \\
& (M_{\mathrm{a}\eta}+M_{\mathrm{a}\eta'})F_1(\phi)F_1'(\phi)\left[\xi_{\mathrm{u}}C_2-\xi_{\mathrm{t}}\left(C_3+2C_4-\frac{1}{2}C_9+\frac{1}{2}C_{10}\right)\right]- \\
& (M_{\mathrm{a}\eta}+M_{\mathrm{a}\eta'})F_2(\phi)F_2'(\phi)\xi_{\mathrm{t}}\left(C_4-\frac{1}{2}C_{10}\right)- \\
& \left(M_{\mathrm{a}\eta}^{P1}+M_{\mathrm{a}\eta'}^{P1}\right)F_1(\phi)F_1'(\phi)\xi_{\mathrm{t}}\left(C_5-\frac{1}{2}C_7\right)- \\
& \left(M_{\mathrm{a}\eta}^{P2}+M_{\mathrm{a}\eta'}^{P2}\right)F_1(\phi)F_1'(\phi)\xi_{\mathrm{t}}\left(2C_6+\frac{1}{2}C_8\right)- \\
& \left(M_{\mathrm{a}\eta}^{P2}+M_{\mathrm{a}\eta'}^{P2}\right)F_2(\phi)F_2'(\phi)\xi_{\mathrm{t}}\left(C_6-\frac{1}{2}C_8\right)- \\
& f_{\mathrm{B}}\cdot\left(F_{\mathrm{a}\eta}^{P2}+F_{\mathrm{a}\eta'}^{P2}\right)F_1(\phi)F_1'(\phi)\xi_{\mathrm{t}}\left(a_6-\frac{1}{2}a_8\right),
\end{aligned} \tag{8}$$

$$\begin{aligned}\mathcal{M}(\eta\eta) = \sqrt{2}\Big\{ & F_{e\eta}F_1(\phi)\Big\{\Big[\xi_u a_2-\xi_t\Big(2a_3+a_4-2a_5-\frac{a_7}{2}+\frac{a_9}{2}-\frac{a_{10}}{2}\Big)\Big]f_\eta^d-\xi_t\Big(a_3-a_5+\frac{a_7}{2}-\frac{a_9}{2}\Big)f_\eta^s\Big\}- \\ & F_{e\eta}^{P2}F_1(\phi)\xi_t\Big(a_6-\frac{1}{2}a_8\Big)f_\eta^d+M_{e\eta}F_1(\phi)\Big\{\Big[\xi_u C_2-\xi_t\Big(C_3+2C_4-\frac{1}{2}C_9+\frac{1}{2}C_{10}\Big)\Big]F_1(\phi)- \\ & \xi_t\Big(C_4-\frac{1}{2}C_{10}\Big)F_2(\phi)\Big\}-M_{e\eta}^{P2}F_1(\phi)\xi_t\Big[\Big(2C_6+\frac{1}{2}C_8\Big)F_1(\phi)+\Big(C_6-\frac{1}{2}C_8\Big)F_2(\phi)\Big]+ \\ & M_{a\eta}\Big\{\Big[\xi_u C_2-\xi_t\Big(C_3+2C_4-\frac{1}{2}C_9+\frac{1}{2}C_{10}\Big)\Big](F_1(\phi))^2-\xi_t\Big(C_4-\frac{1}{2}C_{10}\Big)(F_2(\phi))^2\Big\}- \\ & M_{a\eta}^{P1}\xi_t\Big(C_5-\frac{1}{2}C_7\Big)(F_1(\phi))^2-M_{a\eta}^{P2}\xi_t\Big[\Big(2C_6+\frac{1}{2}C_8\Big)F_1(\phi)^2+\Big(C_6-\frac{1}{2}C_8\Big)F_2(\phi)^2\Big]- \\ & F_{a\eta}^{P2}\xi_t\Big(a_6-\frac{1}{2}a_8\Big)(F_1(\phi))^2\cdot f_B\Big\},\end{aligned} \tag{9}$$

where $\xi_u=V_{ub}^*V_{ud}$, $\xi_t=V_{tb}^*V_{td}$, and $F_1^{(\prime)}(\phi)$, $F_2^{(\prime)}(\phi)$ are the mixing factors.

$$F_1(\phi)=\frac{1}{\sqrt{2}}\cos\phi,\quad F_1^{\prime}(\phi)=\frac{1}{\sqrt{2}}\sin\phi,$$
$$F_2(\phi)=-\sin\phi,\quad F_2^{\prime}(\phi)=\cos\phi. \tag{10}$$

The complete decay amplitudes $\mathcal{M}(\pi^+\eta^\prime)$, $\mathcal{M}(\pi^0\eta^\prime)$, $\mathcal{M}(\eta^\prime\eta^\prime)$ can be obtained easily from Eqs. (6), (7) and (9) respectively, by the following replacements: (f_η^d, f_η^s) $\to$ ($f_{\eta^\prime}^d$, $f_{\eta^\prime}^s$), and ($F_1(\phi)$, $F_2(\phi)$) $\to$ ($F_1^\prime(\phi)$, $F_2^\prime(\phi)$). The Wilson coefficients a_i which appeared in the above equations are the combinations of the Wilson coefficients C_i:

$$a_1=C_2+\frac{C_1}{3},\quad a_2=C_1+\frac{C_2}{3},$$
$$a_i=C_i+\frac{C_{i+1}}{3},\quad \text{for}\quad i=3,5,7,9 \tag{11}$$
$$a_i=C_i+\frac{C_{i-1}}{3},\quad \text{for}\quad i=4,6,8,10.$$

The explicit expressions of individual decay amplitude $F_{e\pi}$ and $F_{e\pi}^{P1,P2}$, $M_{e\pi}$ and $M_{e\pi}^{P1,P2}$, $F_{a\pi}$ and $F_{a\pi}^{P1,P2}$, and $M_{a\pi}$ and $M_{a\pi}^{P1,P2}$, as well as those for $B\to\eta^{(\prime)}$ transitions, such as $F_{e\eta_q}$, etc., can be found in Refs. [7, 8].

2.3 Next-to-leading-order contributions

In the following, we will consider the NLO contributions from the vertex corrections, the quark loops and the magnetic penguins[9].

The vertex corrections have been obtained by evaluating the four Feynman diagrams Figs. 2(a)—2(d)[4], which can be included easily by the modification of the Wilson coefficients a_i when we calculate the two factorizable emission diagrams Fig. 1(a) and 1(b).

$$a_i(\mu)\to a_i(\mu)+\frac{\alpha_s(\mu)}{4\pi}C_F\frac{C_1(\mu)}{N_c}V_i(M),$$
$$\text{for}\quad i=1,2, \tag{12}$$
$$a_j(\mu)\to a_j(\mu)+\frac{\alpha_s(\mu)}{4\pi}C_F\frac{C_{j\pm1}(\mu)}{N_c}V_j(M),$$
$$\text{for}\quad j=3-10, \tag{13}$$

where M is the meson emitted from the weak vertex. The explicit expressions of the vertex function $V_i(M)$ can be found for example in Refs. [2, 9].

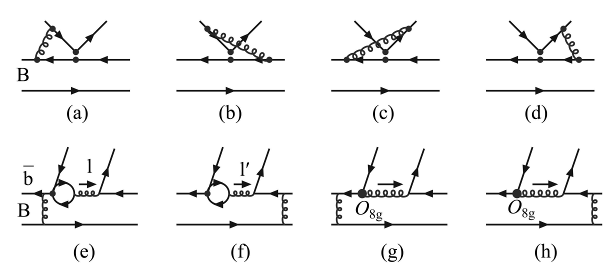

Fig. 2. The typical Feynman diagrams which provide the NLO corrections: the vertex corrections (diagrams a, b, c, d), the quark loops (e, f) and the chromo-magnetic penguins (g, h).

The NLO contribution from the quark loops is a kind of penguin correction with the four quark operators insertion, as illustrated in Figs. 2(e) and 2(f). Here quark-loop contributions from the operators O_{3-6} are included, while those from O_{7-10} are neglected due to their smallness.

For the $b\to d$ transition, the contributions from the various quark loops are given by:

$$\mathcal{H}_{\rm eff}^{(ql)}=-\sum_{q=u,c,t}\sum_{q^\prime}\frac{G_F}{\sqrt{2}}V_{qb}V_{qd}^*\frac{\alpha_s(\mu)}{2\pi}C^{(q)}(\mu,l^2)\times$$
$$\left[\bar{d}\gamma_\rho(1-\gamma_5)T^a b\right](\bar{q}^\prime\gamma^\rho T^a q^\prime), \tag{14}$$

where l^2 is the invariant mass of the gluon, which attaches to the quark loops in Figs. 2(e) and 2(f). The functions $C^{(q)}(\mu,l^2)$ with $q=(u,c,t)$ can be found in Refs. [2, 9].

The NLO quark-loop contribution to the total decay amplitude of the seven considered decays can be generally written as

$$\mathcal{M}^{(ql)}_{M_2M_3}=\langle M_2M_3|\mathcal{H}^{(ql)}_{\rm eff}|B\rangle. \qquad (15)$$

Finally, the chromo-magnetic penguin operator O_{8g} contributes to the considered decays at the NLO level, as shown in Figs. 2(g) and 2(h). In fact, except for these two diagrams, there are also eight other similar diagrams[13], but their contributions are small and have been neglected here. The corresponding weak effective Hamiltonian for the $b\to dg$ transition takes the form of

$$\mathcal{H}^{\rm cmp}_{\rm eff} = -\frac{G_F}{\sqrt{2}}V_{tb}V^*_{td}C_{8g}O_{8g}\,, \qquad (16)$$

with the magnetic-penguin operator O_{8g}

$$O_{8g} = \frac{g}{8\pi^2}m_b\bar{d}_i\sigma_{\mu\nu}(1+\gamma_5)T^a_{ij}G^{a\mu\nu}b_j, \qquad (17)$$

where i,j are the color indices. The corresponding effective Wilson coefficient $C^{\rm eff}_{8g}=C_{8g}+C_5$[12]. At last, the magnetic-penguin corrections to the $B\to\pi\eta^{(\prime)},\eta^{(\prime)}\eta^{(\prime)}$ decays can be generally written as:

$$\mathcal{M}^{(cmp)}_{M_2M_3} = \langle M_2M_3|\mathcal{H}^{\rm cmp}_{\rm eff}|B\rangle. \qquad (18)$$

The decay amplitudes $\mathcal{M}^{(ql)}_{M_2M_3}$ and $\mathcal{M}^{(cmp)}_{M_2M_3}$ are similar in form as those which appeared in Ref. [2].

Following Refs. [2, 14], we here also take $\mu_0=1.0$ GeV as the lower limit of the hard scale t in the evaluation of $C_i(t)$ in the numerical integrations, in order to guarantee the reliability of the perturbative QCD calculations. For more details about this point, one can see the analysis given in Ref. [2].

3 Numerical results and discussions

For the B meson wave function, we adopt the model

$$\phi_B(x,b)=N_Bx^2(1-x)^2\exp\left[-\frac{M_B^2\,x^2}{2\omega_b^2}-\frac{1}{2}(\omega_bb)^2\right], \qquad (19)$$

where ω_b is a free parameter and we take $\omega_b=0.4\pm0.05$ GeV in numerical calculations, and $N_B=101.445$ is the normalization factor for $\omega_b=0.4$ GeV.

For the π and $\eta^{(\prime)}$ mesons, we use the same wave functions and DA's as in Refs. [2, 7, 8]. Other relevant parameters are the following:

$$a_1^\pi = 0,\quad a_2^\pi=0.115\pm0.115,\quad a_4^\pi=-0.015;$$
$$\eta_3 = 0.015,\quad \omega=-3.0,\quad f_q=(1.07\pm0.02)f_\pi,$$
$$f_s = (1.34\pm0.06)f_\pi,\quad \phi=39.3^\circ\pm1.0^\circ, \qquad (20)$$

with $f_\pi=130$ MeV. For the η_q and η_s, we use $a_1^\eta=0$ and $a_2^\eta=0.44\pm0.22$.

The following input parameters[15] will be used in the numerical calculations

$$f_B = 0.21\ {\rm GeV},\ m_\pi=0.14\ {\rm GeV},\ m_\eta=547.5\ {\rm MeV},$$
$$m_{\eta'} = 957.8\ {\rm MeV},\ m_{0\pi}=1.3\ {\rm GeV},\ m_b=4.8\ {\rm GeV},$$
$$M_B = 5.279\ {\rm GeV},\ M_W=80.41\ {\rm GeV},\ \tau_{B^0}=1.527\ {\rm ps},$$
$$\tau_{B^+} = 1.643\ {\rm ps}. \qquad (21)$$

For the relevant CKM matrix elements we use the following values[16]

$$|V_{ud}| = 0.974,\quad |V_{ub}|=4.31\times10^{-3},$$
$$|V_{tb}| = 1.0,\quad |V_{td}|=7.4\times10^{-3}, \qquad (22)$$

with the CKM angle $\alpha=100^\circ\pm20^\circ$.

For a general charmless two-body decays $B\to M\eta^{(\prime)}$, the branching ratio can be written in general as

$$Br(B\to M\eta^{(\prime)}) = \tau_B\frac{1}{16\pi m_B}|\mathcal{M}|^2. \qquad (23)$$

For the considered decay channels the total decay amplitude $\mathcal{M}$ can be written as:

$$\mathcal{M}_{\pi^+\eta^{(\prime)}} = \mathcal{M}(\pi^+\eta^{(\prime)})+\mathcal{M}^{(ql)}_{\pi^+\eta^{(\prime)}}+\mathcal{M}^{(cmp)}_{\pi^+\eta^{(\prime)}}, \qquad (24)$$
$$\mathcal{M}_{\pi^0\eta^{(\prime)}} = \mathcal{M}(\pi^0\eta^{(\prime)})+\mathcal{M}^{(ql)}_{\pi^0\eta^{(\prime)}}+\mathcal{M}^{(cmp)}_{\pi^0\eta^{(\prime)}}, \qquad (25)$$
$$\mathcal{M}_{\eta^{(\prime)}\eta^{(\prime)}} = \mathcal{M}(\eta^{(\prime)}\eta^{(\prime)})+\mathcal{M}^{(ql)}_{\eta^{(\prime)}\eta^{(\prime)}}+\mathcal{M}^{(cmp)}_{\eta^{(\prime)}\eta^{(\prime)}}. \qquad (26)$$

The contributions from vertex corrections have been absorbed into the re-definition of the Wilson coefficients.

Using the wave functions and the input parameters as specified in previous subsection, it is straightforward to calculate the CP-averaged branching ratios for these seven considered decays, which are listed in Table 2. For comparison, we also list the corresponding experimental results[15] and numerical results evaluated in the framework of the QCDF approach[6]. The error of the pQCD predictions for the branching ratios is the combination of the uncertainties of parameter $\omega_b=0.4\pm0.04$ GeV, the CKM angle $\alpha=100^\circ\pm20^\circ$ and the Gegenbauer coefficients $a_2^\pi=0.115\pm0.115$ and $a_2^\eta=0.44\pm0.22$.

Table 1. The pQCD predictions for the branching ratios (in units of 10^{-6}). The label +VC, +QL, +MP and NLO means the inclusion of the vertex corrections, the quark loops, the magnetic penguin, and all the considered NLO corrections, respectively.

mode	LO	+VC	+QL	+MP	NLO	data[15]	QCDF[6]
$B^+\to\pi^+\eta$	4.3	4.1	4.5	4.2	$4.1^{+1.3}_{-1.1}$	4.4 ± 0.4	$4.7^{+2.7}_{-2.3}$
$B^+\to\pi^+\eta'$	2.6	2.8	2.5	2.7	$2.8^{+0.9}_{-0.7}$	$2.7^{+0.6}_{-0.5}$	$3.1^{+1.9}_{-1.7}$
$B^0\to\pi^0\eta$	0.14	0.20	0.13	0.13	$0.19^{+0.04}_{-0.06}$	<1.5	$0.28^{+0.48}_{-0.28}$
$B^0\to\pi^0\eta'$	0.05	0.15	0.08	0.07	$0.15^{+0.05}_{-0.03}$	1.2 ± 0.4	0.17
$B^0\to\eta\eta$	0.17	0.09	0.11	0.07	$0.09^{+0.06}_{-0.05}$	<1.4	$0.16^{+0.45}_{-0.19}$
$B^0\to\eta'\eta$	0.22	0.60	0.11	0.09	$0.59^{+0.39}_{-0.26}$	<1.2	$0.16^{+0.61}_{-0.18}$
$B^0\to\eta'\eta'$	0.04	0.08	0.03	0.02	$0.08^{+0.05}_{-0.04}$	<2.1	$0.06^{+0.25}_{-0.07}$

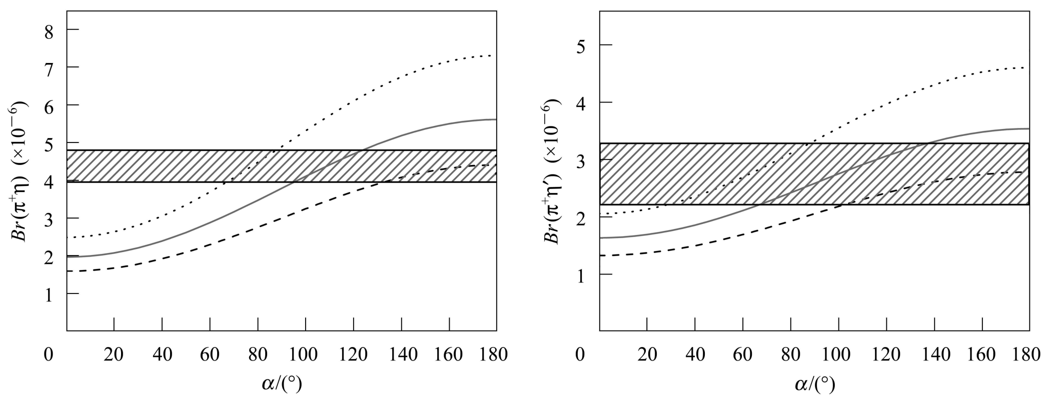

Fig. 3. The α dependence of the branching ratios (in units of 10^{-6}) of $B^+\to\pi^+\eta^{(\prime)}$ decays for $\omega_b = 0.36$ GeV (dotted curve), 0.40 GeV (solid curve) and 0.44 GeV (dashed curve).

From the numerical results as listed in Table 1 and shown in Fig. 3, one can see that:

1) For the two charged channels, the NLO contributions are small in size. The NLO pQCD predictions agree very well with the data and the QCDF predictions.

2) For $B\to\pi^0\eta'$ decay, the NLO pQCD prediction agrees well with the QCDF one, but it is rather different from the measured value. Of course, the error of the measured value is still large. This difference will be tested by the forthcoming LHC experiments.

3) For the remaining four neutral decays, the NLO pQCD predictions are generally consistent with the QCDF predictions and the data with one standard deviation.

4) For $B\to\eta\eta'$ decay, the NLO contributions are large. The central value of the NLO pQCD prediction is also rather different from the QCDF one, also to be tested by the LHC experiments.

Now we turn to the evaluations of the CP-violating asymmetries of $B\to\pi\eta^{(\prime)},\eta^{(\prime)}\eta^{(\prime)}$ decays in pQCD approach. The direct and mixing induced CP violating asymmetries for the considered decays are defined in the same way as in Refs. [2, 7, 8]. The numerical results for the direct CP-violating asymmetries are listed in Table 2. For comparison, we also show the available data[15] and the QCDF predictions[6].

Table 2. The pQCD predictions for the direct CP violating asymmetries (in units of percent). The errors for the NLO results correspond to the uncertainties of ω_b, CKM angle (α) and Gegenbauer coefficients (a_2^{π}, a_2^{η}), respectively.

mode	LO	+VC	+QL	+MP	NLO	data	QCDF
$B^+\to\pi^+\eta$	−23.4	−21.6	−19.4	−22.8	$-18.4^{+3.2+4.3+1.4}_{-3.5-3.4-0.7}$	-19 ± 7	−14.9
$B^+\to\pi^+\eta'$	34.2	47.4	−29.7	−33.2	$-46.0^{+3.6+9.7+2.4}_{-2.5-6.3-1.8}$	15 ± 15	−8.6
$B^0\to\pi^0\eta$	−65.1	−57.9	−58.1	−58.5	$-62.4^{+6.5+5.2+1.0}_{-2.9-0.0-11.1}$	–	−17.9
$B^0\to\pi^0\eta'$	−79.6	−38.0	−59.0	−65.2	$-35.1^{+2.2+3.8+5.9}_{-2.9-0.0-5.8}$	–	−19.2
$B^0\to\eta\eta$	85.8	74.0	71.2	71.2	$61.7^{+5.9+11.2+3.7}_{-0.0-7.1-0.0}$	–	63^{+32}_{-74}
$B^0\to\eta'\eta$	52.3	44.9	13.4	−13.1	$33.8^{+0.0+15.5+4.7}_{-7.6-8.3-0.8}$	–	56^{+32}_{-144}
$B^0\to\eta'\eta'$	62.8	48.1	31.5	15.3	$41.8^{+2.6+17.3+4.5}_{-0.0-10.9-4.8}$	–	46^{+43}_{-147}

From the pQCD predictions and currently available experimental measurements for the CP violating asymmetries of the $B \to \pi\eta^{(\prime)}, \eta^{(\prime)}\eta^{(\prime)}$ decays, one can see the following points:

1) The pQCD prediction for $\mathcal{A}_{CP}^{\rm dir}(B^+ \to \pi^+\eta)$ agrees perfectly with both the data and the QCDF prediction. The agreement between the pQCD result and the measured value is improved effectively by the inclusion of the NLO contributions.

2) For $\mathcal{A}_{CP}^{\rm dir}(B^+ \to \pi^+\eta')$, however, the pQCD prediction has the same sign as the QCDF one, but it is much larger than the latter in magnitude. The corresponding experimental measurement is currently still poor.

3) For the remaining five neutral decays, experimental measurements are still absent. The size of the pQCD predictions for the direct CP-violating asymmetries becomes small effectively when the NLO contributions are included, and approaches the QCDF predictions for the three $B^0 \to \eta^{(\prime)}\eta^{(\prime)}$ decays.

4) For $\mathcal{A}_{CP}(B^0 \to \pi^0\eta^{(\prime)})$, unfortunately, the differences between the pQCD predictions and the QCDF ones are still large.

5) It is worth mentioning that the theoretical uncertainties of pQCD and QCDF predictions for CP-violating asymmetries are still large at present.

4 Summary

In this paper, we calculated the branching ratios and CP-violating asymmetries of the seven $B \to (\pi, \eta^{(\prime)})\eta^{(\prime)}$ decays in the pQCD factorization approach. The partial NLO contributions considered here include the QCD vertex corrections, the quark-loops and the chromo-magnetic penguins.

From our calculations and phenomenological analysis, we found the following results:

(a) Except for $B^0 \to \pi^0\eta'$ decays, the NLO pQCD predictions for the branching ratios of the considered decays agree very well with the data and the QCDF results.

(b) For $Br(B^0 \to \pi^0\eta')$, the pQCD prediction agrees very well with the QCDF prediction, but it is rather different from the measured value, although the experimental error is still large. Such differences will be tested in the LHC experiments.

(c) The NLO pQCD prediction for $\mathcal{A}_{CP}^{\rm dir}(B^+ \to \pi^+\eta)$ agrees perfectly with both the data and the QCDF prediction. The theoretical uncertainties of the CP-violating asymmetries are still large, and the data for the other six considered decays are poor or absent at present.

References

1 Charng Y Y, Kurimoto T, LI H N. Phys. Rev. D, 2006, **74**: 074024
2 XIAO Z J, ZHANG Z Q, LIU X, GUO L B. Phys. Rev. D, 2008, **78**: 114001
3 Ali A, Kramer G, LÜ C D. Phys. Rev. D, 1998, **58**: 094009
4 Beneke M, Buchalla G, Neubert M, Sachrajda C T. Phys. Rev. Lett., 1999, **83**: 1914; Nucl. Phys., 2000, **591**: 313
5 DU D S, GONG H J, SUN J F, YANG D S, ZHU G H. Phys. Rev. D, 2002, **65**: 074001; SUN J F, ZHU G H, DU D S. Phys. Rev. D, 2003, **68**: 054003
6 Beneke M, Neubert M. Nucl. Phys., 2003, **675**: 333
7 LIU X, WANG H S, XIAO Z J, GUO L B, LÜ C D. Phys. Rev. D, 2006, **73**: 074002; WANG H S, LIU X, XIAO Z J, GUO L B, LÜ C D. Nucl. Phys., 2006, **738**: 243
8 XIAO Z J, GUO D Q, CHEN X F. Phys. Rev. D, 2007, **75**: 014018
9 LI H N, Mishima S, Sanda A I. Phys. Rev. D, 2005, **72**: 114005
10 LÜ C D, Ukai K, YANG M Z. Phys. Rev. D, 2001, **63**: 074009
11 Keum Y Y, LI H N, Sanda A I. Phys. Rev. D, 2001, **63**: 054008; Kurimoto T, LI H N, Sanda A I. Phys. Rev. D, 2001, **65**: 014007
12 Buchalla G, Buras A J, Lautenbacher M E. Rev. Mod. Phys., 1996, **68**: 1125
13 Mishima S, Sanda A I. Prog. Theor. Phys., 2003, **110**: 549
14 ZHANG Z Q, XIAO Z J. Eur. Phys. J., 2009, **59**; ZHANG Z Q, XIAO Z J, 2008,arXiv: 0807.2024[hep-ph]; LIU J, ZHOU R, XIAO Z J. 2008, arXiv: 0812.2132[hep-ph]
15 Heavy Flavor Averaging Group, Barberio E et al. hep-ex/0808.1297v1; online update at http://www.slac.stanford.edu/xorg/hfag
16 Particle Data Group (YAO W M et al.). J. Phys. G., 2006, **33**: 1